J. Appl. Comput. Mech., 6(2) (2020) 219-234
DOI: 10.22055/JACM.2019.28965.1527

ISSN: 2383-4536
jacm.scu.ac.ir

M&MoCS
Shahid Chamran University of Ahvaz

Journal of
Applied and Computational Mechanics

Research Paper

Efficient Solution of Nonlinear Duffing Oscillator

Iman Khatami[1], **Ehsan Zahedi**[2], **Mohsen Zahedi**[3]

[1] Department of Mechanical Engineering, Chabahar Maritime University, Iran, Email: Iman.Khatami81@gmail.com
[2] Department of Biosystems Engineering, Shiraz University, Iran, Email: Zahedi_Ehsan@yahoo.com
[3] Faculty of Computer Engineering, University of Isfahan, Iran, Email: Seyyed.Mohsen.Zahedi@gmail.com

Received March 18 2019; Revised April 25 2019; Accepted for publication May 17 2019.
Corresponding author: Ehsan Zahedi (Zahedi_Ehsan@yahoo.com)

Abstract. In this paper, the efficient multi-step differential transform method (EMsDTM) is applied to get the accurate approximate solutions for strongly nonlinear duffing oscillator. The main improvement of EMsDTM which is to reduce the number of arithmetic operations, is thoroughly investigated and compared with the classic multi-step differential transform method (MsDTM). To illustrate the applicability and accuracy of the new method, six case studies of the free undamped and forced damped conditions are considered. The periodic response curves of both MsDTM and EMsDTM methods are obtained and contrasted with the exact solution or the numerical solution of Runge Kutta 4th order (RK4) method. This approach can be easily extended to other nonlinear systems and therefore is widely applicable in engineering and other sciences.

Keywords: Efficient multi-step transforms method, Duffing oscillator, Nonlinear equation, Differential transformation method.

1. Introduction

A Duffing oscillator consists of a beam placed vertically between two magnets with the top end fixed and the bottom end free to swing. By applying velocity to the beam, it oscillates between the two magnets. The schematic of a duffing oscillator is shown in Fig.1. This periodically forced oscillator with a nonlinear elasticity represents the dynamics of many mechanical structures in physical science and practical engineering research [1-2]. Many scientists are inspired by nonlinear differential Duffing equations to replicate similar dynamics in the natural world [3-4].
The nonlinear Duffing equation is presented as follows:

$$\frac{d^2x(t)}{dt^2} + \rho_1 x(t) + \mu\frac{dx(t)}{dt} + \rho_3 x(t)^3 + \rho_5 x(t)^5 + \cdots + \rho_n x(t)^n = f cos\Omega t, \tag{1}$$

where ρ_1 is the linear stiffness coefficient, $\rho_3, \rho_5, \ldots, \rho_n$ are the nonlinear arbitrary constants in the restoring force, and μ represents the damping parameter. Also, f is the amplitude and Ω is the angular frequency of the periodic driving force. Due to the presence of strong nonlinearity terms, a wide range of dynamic response such as periodic oscillations and chaotic dynamic behavior can be recorded in the oscillation.
There are many types of Duffing equation, for instance, the Duffing–harmonic equation [5] and the cubic–quintic Duffing equation [6]. In particular, the cubic–quintic Duffing equation is found in the modeling of free vibrations of a restrained uniform beam with intermediate lumped mass [7], the generalized compound Korteweg–de Vries (KdV) equation in nonlinear wave systems [8], the generalized Pochhammer–Chree (PC) equations [9], the nonlinear dynamics of a slender elastic [10], or the propagation of a short electromagnetic pulse in a nonlinear medium [11].

Published online: August 28 2019

By assigning n equal to 5 and setting $f = \mu = 0$, Eq. (1) turns to the free undamped cubic-quintic Duffing oscillator as follows:

$$\frac{d^2x(t)}{dt^2} + \rho_1 x(t) + \rho_3 x(t)^3 + \rho_5 x(t)^5 = 0. \tag{2}$$

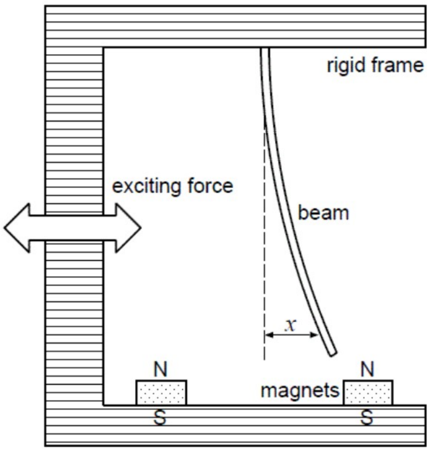

Fig. 1. Mechanical interoperation of Duffing oscillator after [4]

By adding damping part to the left side and harmonic excited force to the right hand side of Eq. (2) the damped forced cubic-quintic Duffing oscillators is generated as:

$$\frac{d^2x(t)}{dt^2} + \rho_1 x(t) + \mu\frac{dx(t)}{dt} + \rho_3 x(t)^3 + \rho_5 x(t)^5 = fcos\Omega t. \tag{3}$$

It is obvious that in the condition of $\mu = \rho_3 = \rho_5 = 0$, the Duffing equation is changed to a simple harmonic oscillator. Duffing oscillators have received remarkable attention in recent decades due to the variety of their engineering applications [12-14]. The presence of the high power nonlinear term in the Duffing equation makes it challenging to determine the closed-form solution. There are many analytical and numerical methods for obtaining good approximation solutions of nonlinear differential equations [15-17]. One well-known analytical practice for solving nonlinear equations is the perturbation technique. Several methods in this family such as the variation iteration method (VIM) [18], the homotopy perturbation method (HPM) [19-21], the homotopy analyzed method (HAM) [22], and the Adomian decomposition method (ADM) [23] have been developed to solve nonlinear equations. Lai et al. [24] and Guo et al. [25] use the harmonic balance method and iterative homotopy harmonic balance method, respectively, to estimate nonlinear oscillation. Khan et al. [26] couple the homotopy perturbation method with a variational formulation approach to set up a fourth-order approximation of a nonlinear oscillation. However, their trail functions do not satisfy the initial conditions. Farzaneh et al. [27] used global error minimization (GEM) to obtain an approximate closed-form analytical solution for nonlinear oscillation differential equations. Principally, perturbation methods are useful when small parameters exist in nonlinear systems where the solution can be analytically expanded into a power series of the parameters.

Elias-Zuniga derived the exact solution of the following cubic-quintic Duffing oscillator by applying Jacobi elliptic functions [28]:

$$\frac{d^2x(t)}{dt^2} + Ax(t) + Bx(t)^3 + Cx(t)^5 = 0, \tag{4}$$

where A, B and C represent constant parameters of the system. The closed-form solution is assumed to be in the form of:

$$x^2(t) = \frac{1}{a + bcn^2(\omega t + \varphi, k^2)}, \tag{5}$$

where a, b, k, ω and φ are unknown parameters that need to be determined. Here $cn(\omega t + \varphi, k^2)$ is the cn Jacobian elliptic function that has a period in ωt equal to $4K(k^2)$, and $K(k^2)$ is the complete elliptic integral of the first kind for modulus k. By considering initial conditions of $x(0) = x_0$ and $x'(0) = 0$, the unknown parameters are determined by:

$$\begin{cases} a = -\dfrac{4C}{3B + 2Cx_0 \pm (\sqrt{3} \times \sqrt{-16AC + (B - 2Cx_0^2)(3B + 2Cx_0^2)})} \\ b = \dfrac{1 - ax_0^2}{x_0^2} \\ k^2 = \dfrac{(2A + Bx_0^2 - 2a^2Ax_0^4 - aBx_0^4)}{2A + 4aAx_0^2 + 2B^2x_0^2 + aBx_0^4} \\ \omega^2 = -\dfrac{(2A + 4aAx_0^2 + 2Bx_0^2 + aBx_0^4)}{2(1 + ax_0^2 + a^2x_0^4)} \end{cases}. \tag{6}$$

The details of the solution are well-presented in Elias-Zuniga's research [28]. Since his exact solution is limited to a free undamped cubic-quintic Duffing oscillator, in this study, the closed-form solution (Eq. (5)) is applied for contrast with relevant examples of the proposed method. The rest four case studies are compared with RK4 numerical solutions.

The differential transform method (DTM) is a useful method based on the Taylor series expansion for solving linear and nonlinear equations with known initial and boundary condition values [29]. This method has the limitation of convergence. In fact, divergence from the exact solution arises when independent variable values are far from the center of the Taylor series. To overcome this limitation, a multi-step differential transform method (MsDTM) is applied [30-32]. In this method, the interval of independent variables is divided into subintervals. Therefore, the center of the series changes for each subinterval and independent variable values are no longer far from the center of the series. The MsDTM algorithm accelerates the convergence of the series solutions over a large domain and improves the accuracy of the results compared with DTM. The method applies in a direct way without using linearization, perturbation or restrictive assumptions. The validity of this technique is verified through illustrative examples of non-chaotic and chaotic systems [33].

Although MsDTM can overcome the convergence problem of DTM, it requires too many subintervals. To remedy this, in this research an efficient MsDTM (EMsDTM) is applied to solve the generalized Duffing equation with high nonlinearity. In MsDTM, the polynomial functions are applied to obtain the solution in each subinterval while in EMsDTM, the solution is achieved by the use of trigonometric functions which leads to a significant increase in the quality of the results. EMsDTM provides solutions in terms of convergent series with easily computable components. The approach yields simple nonlinear algebraic equations instead of nonlinear differential equations without analytical solutions. These approximate solutions are valid for small as well as large amplitudes of oscillation. This method is very efficient, accurate and can be used to provide analytical solutions for nonlinear systems of differential equations.

The paper is organized as follows: in Section 2, the fundamental formulations of DTM and MsDTM are described; the basic principle of EMsDTM is explored in Section 3; and in Section 4, the EMsDTM is implemented successfully to solve Duffing oscillation systems in six scenarios. To verify the accuracy of the proposed method the exact solution and numerical approximations are used.

2. Concept of DTM and MsDTM

The Taylor series of an analytic function $x(t)$ around point t_0 is expressed by:

$$x(t) = \textstyle\sum_{k=0}^{\infty} X[k](t - t_0)^k, \tag{7}$$

where $X[k]$ is the transformed function of $x(t)$, defined as:

$$X[k] = \frac{1}{k!}\left[\frac{d^k x(t)}{dt^k}\right]_{t=t_0}. \tag{8}$$

Substituting Eq. (8) into Eq. (7) yields:

$$x(t) = \sum_{k=0}^{\infty} \frac{(t - t_0)^k}{k!}\left[\frac{d^k x(t)}{dt^k}\right]_{t=t_0}. \tag{9}$$

A finite number of summations in Eq. (9) provides a good approximation of $x(t)$. Therefore, Eq. (9) is expressed as:

$$x(t) = \textstyle\sum_{k=0}^{N} \frac{(t-t_0)^k}{k!}\left[\frac{d^k x(t)}{dt^k}\right]_{t=t_0}, \tag{10}$$

where N represents the finite number of terms providing the approximation of $x(t)$. Table 1 shows some basic transformation functions used in this paper.

Table1. Differential transform operations

Original Function	Transformed Function
$ax(t) \pm by(t)$	$aX(t) \pm bY(t)$
$x(t)y(t)$	$\sum_{l=0}^{k} X(l)Y(k-l)$
$x(t)y(t)z(t)$	$\sum_{s=0}^{k}\sum_{m=0}^{k-s} X(s)Y(m)Z(k-s-m)$
$\frac{d^m x(t)}{dt^m}$	$\frac{(k+m)!}{k!}X(k+m)$
$\cos(\omega(t)+\alpha)$	$\frac{\omega^k}{k!}\cos(\omega(t)+\alpha)$
$x_1(t), x_2(t), \cdots x_n(t)$	$X[k] = \sum_{k_{n-1}=0}^{k}\sum_{k_{n-2}=0}^{k_{n-1}} \cdots \sum_{k_2=0}^{k_3}\sum_{k_1=0}^{k_2} G_1[k_1]G_2[k_2-k_1]\, G_{n-1}[k_{n-1}-k_{n-2}]G_n[k-k_{n-1}]$

In MsDTM the whole domain is divided into some finite subintervals to increase the accuracy, then for each subinterval the DTM is applied. The nonlinear differential equation is considered to be:

$$g\left(t, x(t), x'(t), x''(t), x'''(t), \cdots x^{(p)}(t)\right), \qquad t \in \left[t_f, t_l\right], \tag{11}$$

where p is the highest order of derivation and t_f and t_l are the first and last points of the interval, respectively. The initial conditions are:

$$x^{(q)}\left(t_f\right) = C_q, \qquad q = 0, 1, 2, \cdots, p-1, \tag{12}$$

where C_q is a real number. According to eq. (7) and eq. (10), $x(t)$ is revised to:

$$x(t) = \sum_{i=0}^{N} X[\mathrm{i}](t-t_0)^{\mathrm{i}} \qquad t\epsilon\left[t_f, t_l\right]. \tag{13}$$

where $X[\mathrm{i}]$ is a transformed function, and N is the number of terms selected by the convergence test. As $x^{(q)}\left(t_f\right) = X[q]$, the initial conditions are rewritten as:

$$X[q] = C_q, \qquad q = 0, 1, 2, \cdots, p-1 \tag{14}$$

By dividing the t variable into T subinterval parts, $\left[t_f, t_l\right]$ is distributed into equal parts h, as follows:

$$h = \frac{t_f - t_l}{T}, \qquad T = 1, 2, 3, \cdots, p-1, \tag{15}$$

where T is the number of subintervals. By this technique for each subinterval, a distinct function is defined. These functions are the solutions of MsDTM:

$$x(t) = \begin{cases} x_1(t) = \sum_{i=0}^{N} X_1[\mathrm{i}](t-t_0)^{\mathrm{i}} & t\epsilon[t_1, t_2], \\ x_2(t) = \sum_{i=0}^{N} X_2[\mathrm{i}](t-t_2)^{\mathrm{i}} & t\epsilon[t_2, t_3], \\ x_3(t) = \sum_{i=0}^{N} X_3[\mathrm{i}](t-t_3)^{\mathrm{i}} & t\epsilon[t_3, t_4], \\ \vdots & \vdots, \\ x_{T-1}(t) = \sum_{i=0}^{N} X_{T-1}[\mathrm{i}](t-t_{T-1})^{\mathrm{i}} & t\epsilon[t_{T-1}, t_T], \\ x_T(t) = \sum_{i=0}^{N} X_T[\mathrm{i}](t-t_T)^{\mathrm{i}} & t\epsilon\left[t_T, t_f\right], \end{cases} \tag{16}$$

It is clear that the initial condition of $x_1(t)$ is $x_1^{(q)}(t_f) = X(q)$ and of $x_2(t)$ is $x_2^{(q)}(t_2) = x_1^{(q)}(t_2)$. As the value of $x_1^{(q)}(t_2)$ is calculated in the first subinterval, $x_2^{(q)}(t_2)$ is already known. By continuing the procedure the initial value of each subinterval is computed.

3. Concept of EMsDTM

The drawback of MsDTM is that in order to have accurate results there needs to be a large number of subintervals. EMsDTM overcomes this drawback by considerably decreasing the number of subintervals while the accurate results are maintained [33]. By dividing $[t_f, t_l]$ into L subintervals, for each subinterval $[t_j, t_{j+1}]$, $x_j(t)$ is defined as:

$$x_j(t) = \sum_{\alpha=0}^{N} X_j[\mathrm{i}](t-t_j)^{\mathrm{i}} = X_j[0] + X_j[1](t-t_j)^1 + X_j[2](t-t_j)^2 + \cdots + X_j[N](t-t_j)^{\mathrm{N}}. \tag{17}$$

$x_j(t)$ can also be denoted as:

$$x_j(t) = \sum_{l=0}^{m} \propto_{jl} \cos\left(\beta_{jl}(t-t_j)\right) + \sum_{l=0}^{m} \delta_{jl} \sin\left(\varepsilon_{jl}(t-t_j)\right), \tag{18}$$

where $j = 1, 2, \dots, L$ and $\propto_{jl}$, β_{jl} , δ_{jl} , ε_{jl} are the unknown parameters that need to be found. These parameters can be real or imaginary. Although increasing the number m gives results that are more precise, assigning m a value equal to 3 or even 2 provides sufficiently accurate results. Equation (18) is revised according to the the Taylor series of sine and cosine as follows:

$$x_j(t) = \sum_{l=0}^{m} \propto_{jl} \left(1 - \frac{\beta_{jl}(t-t_j)^2}{2!} + \frac{\beta_{jl}(t-t_j)^4}{4!} - \frac{\beta_{jl}(t-t_j)^6}{6!} + \cdots\right) + \sum_{l=0}^{m} \delta_{jl} \left(\frac{\beta_{jl}(t-t_j)^3}{3!} + \frac{\beta_{jl}(t-t_j)^5}{5!} - \frac{\beta_{jl}(t-t_j)^7}{7!} + \cdots\right) \tag{19}$$

By comparing the odd and even powers of Eq. (17) and Eq. (19), the following results are given:

$$\begin{cases} X_j[0] = \sum_{l=0}^{m} \propto_{jl} \\ X_j[2] = \frac{-1}{2!}\sum_{l=0}^{m} \propto_{jl} \beta_{jl}{}^2 \\ X_j[4] = \frac{1}{4!}\sum_{l=0}^{m} \propto_{jl} \beta_{jl}{}^4 \\ X_j[6] = \frac{-1}{6!}\sum_{l=0}^{m} \propto_{jl} \beta_{jl}{}^6 \\ X_j[8] = \frac{1}{8!}\sum_{l=0}^{m} \propto_{jl} \beta_{jl}{}^8 \\ \vdots \end{cases} \tag{20}$$

$$\begin{cases} X_j[1] = \sum_{l=0}^{m} \delta_{jl}\varepsilon_{jl} \\ X_j[3] = \frac{-1}{3!}\sum_{l=0}^{m} \delta_{jl}\varepsilon_{jl}{}^3 \\ X_j[5] = \frac{1}{5!}\sum_{l=0}^{m} \delta_{jl}\varepsilon_{jl}{}^5 \\ X_j[7] = \frac{-1}{7!}\sum_{l=0}^{m} \delta_{jl}\varepsilon_{jl}{}^7 \\ X_j[9] = \frac{1}{9!}\sum_{l=0}^{m} \delta_{jl}\varepsilon_{jl}{}^9 \\ \vdots \end{cases}, \tag{21}$$

where $j = 1, 2, 3 \dots L$. Advanced mathematical software (Maple 18) is used to solve the nonlinear algebraic systems of equations (19- 21) to derive the $\propto_{jl}$, β_{jl} , δ_{jl} and ε_{jl} parameters. Subsequently, $x_j(t)$ is calculated for each subinterval. Furthermore, the initial condition of step $j+1$ is determined from $x_j(t)$.

4. Solutions of Duffing Oscillator

In this section MsDTM and EMsDTM, which are presented in Sections 2 and 3 are applied to nonlinear Duffing oscillators, and the accuracy and number of subintervals are compared. Six case studies are chosen to investigate the reliability of proposed method. Table 2 shows the parameters of the selected cases.

Table 2. Parameters of the selected case studies

Case study	Parameters
1	$\rho_1=1, \mu=0, \rho_3=10, \rho_5=1,\ \rho_7=0, \rho_9=0$
2	$\rho_1=1, \mu=0, \rho_3=10, \rho_5=1, \rho_7=1, \rho_9=0,\ \ A=0.1$
3	$\rho_1=1, \mu=0, \rho_3=1, \rho_5=1, \rho_7=0.1,\ \ \rho_9=0, A=1$
4	$\rho_1=1, \mu=0, \rho_3=10, \rho_5=10, \rho_7=10, \rho_9=5$
5	$\rho_1=1, \mu=0.01, \rho_3=10, \rho_5=1, \rho_7=0, \rho_9=0$
6	$\rho_1=1, \mu=0.01,\ \rho_3=0.1, \rho_5=0.1, \rho_7=0, \rho_9=0, f=0.01, \Omega=1$

4.1. Free Undamped vibrations

By setting n equal to nine and $f=\mu=0$ in the Eq. (1), the following Duffing equation is generated:

$$\frac{d^2x(t)}{dt^2}+\rho_1x(t)+\rho_3x(t)^3+\rho_5x(t)^5+\rho_7x(t)^7+\rho_9x(t)^9=0. \tag{22}$$

According to Table 1 and Eq. (16), the differential transformation of Eq. (22), for each subinterval is:

$$\begin{aligned}X_j[i+2]=&-\frac{1}{(i+2)(i+1)}\Bigg(X_j[i]+\rho_3\sum_{k_2=0}^{i}\sum_{k_1=0}^{k_2}X_j[k_1]X_j[k_2-k_1]X_j[i-k_2]\\&+\rho_5\sum_{k_4=0}^{i}\sum_{k_3=0}^{k_4}\sum_{k_2=0}^{k_3}\sum_{k_1=0}^{k_2}X_j[k_1]X_j[k_2-k_1]X_j[(k_3-k_2)]X_j[(k_4-k_3)]X_j[(i-k_4)]\\&+\rho_7\sum_{k_6=0}^{i}\sum_{k_5=0}^{k_6}\sum_{k_4=0}^{k_5}\sum_{k_3=0}^{k_4}\sum_{k_2=0}^{k_3}\sum_{k_1=0}^{k_2}X_j[k_1]X_j[(k_2-k_1)]X_j[(k_3-k_2)]X_j[(k_4-k_3)]X_j[(k_5\\&-k_4)]\,X_j[(k_6-k_5)]X_j[(i-k_6)]\\&+\rho_9\sum_{k_8=0}^{i}\sum_{k_7=0}^{k_8}\sum_{k_6=0}^{k_7}\sum_{k_5=0}^{k_6}\sum_{k_4=0}^{k_5}\sum_{k_3=0}^{k_4}\sum_{k_2=0}^{k_3}\sum_{k_1=0}^{k_2}X_j[k_1]X_j[(k_2-k_1)]X_j[(k_3-k_2)]X_j[(k_4-k_3)]X_j[(k_5\\&-k_4)]\,X_j[(k_6-k_5)]X_j[(k_7-k_6)]X_j[(k_8-k_7)]X_j[(i-k_8)]\Bigg),\end{aligned} \tag{23}$$

where $i=0,1,2,\dots,N$ and $j=0,1,2,\dots,T$. The differential transformation of the initial conditions are $X_1[0]=1$ and $X_1[1]=0$. The initial condition for each subinterval is defined as:

$$X_j[0]=x_{j-1}(t) \qquad \text{at} \qquad t=t_j, \qquad j=1,2,\dots,L \tag{24}$$

$$X_j[1]=\frac{dx_{j-1}(t)}{dt} \qquad \text{at} \qquad t=t_j, \qquad j=1,2,\dots,L \tag{25}$$

$t\epsilon\left[t_f\ t_l\right]$ is divided into T subintervals of equal size h, where $h=\frac{t_f-t_l}{T}$. In order to see applicability and accuracy of EMsDTM, the different values of $n,\ \rho_3,\ \rho_5, \rho_{7,}, \rho_9$ are considered in the following sections.

4.1.1. Free undamped cubic-quintic Duffing oscillator

Equation (22) turns to the free undamped cubic-quintic Duffing oscillator by selecting $\rho_1=1,\ \rho_3=10,\ \rho_5=1, \rho_7=\rho_9=0$. It set as a case study 1. According to Eq. (16), by assigning $h=0.8\ (t_{j+1}=t_j+h)$, $X_j[\mathrm{i}]$ will calculate where $i=0,1,2,\dots,N$ and $j=1,2,3,\dots,T$. Table 3 displays the values of $X_j[\mathrm{i}]$ for each subinterval.

Table 3. The values of $X_j[i]$ for each subinterval based on MsDTM for case study 1

	$i=0$	$i=1$	$i=2$	$i=3$	...	$i=10$	$t\epsilon[t_j\ t_{j+1}]$
$j=1$	0.1	0	−0.055005	0	...	−0.000010	$t\epsilon[0\ \ 0.8]$
$j=2$	0.067103	−0.076787	−0.035063	0.014527	...	−0.000006	$t\epsilon[0.8\ \ 1.6]$
$j=3$	−0.008688	−0.102102	−0.004347	0.017055	...	$-5.01196e-7$	$t\epsilon[1.6\ \ 2.4]$
⋮	⋮	⋮	⋮	⋮	⋮		⋮
$j=L=124$	0.0084780	−0.102119	−0.004242	+0.0170566	...	$4.883101e-7$	$t\epsilon[98.4\ \ 100]$

According to Eq. (15), $x_1(t)$ for $t\epsilon[0\ \ 0.8]$ is given by:

$$x_1(t) = 0.1 - 0.05500500000t^2 + 0.005961166875t^4 - 0.0005619801033\,t^6 + 0.00007831469173t^8 - 0.00001051067386t^{10} \tag{26}$$

This procedure is continued for all subintervals to compute $x_2(t), x_3(t), x_4(t), \dots, x_T(t)$. These terms of $x(t)$ are the approximation solution. To obtain a precise solution based on MsDTM, the h parameter needs to be set appropriately. Figure 2 shows the effect of subinterval h on the accuracy of MsDTM and EMsDTM. By choosing $h = 0.8$ where the number of subintervals in $t \in [0\ 100]$ leads to $T = 124$, MsDTM derives a close match to the closed-form solution. As shown in Fig. 1 the subinterval h for EMsDTM can reach 50 which decreases the arithmetic operation significantly.

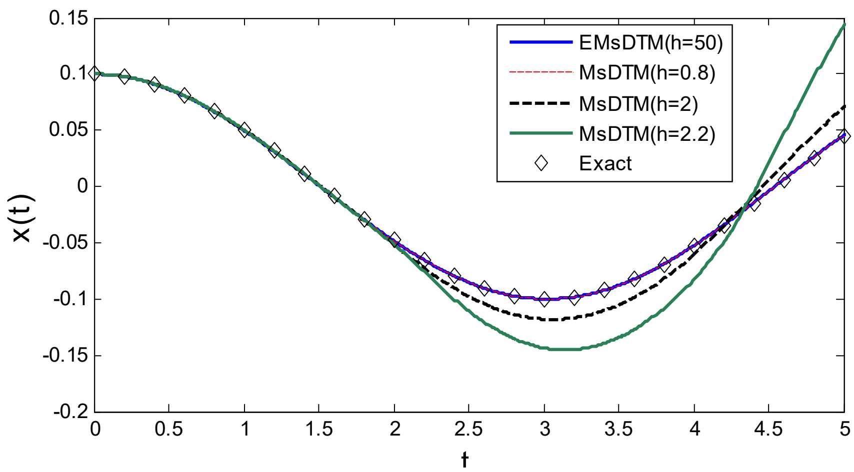

Fig. 2. Effect of subinterval h on result accuracy of MsDTM and EMsDTM for case study 1

The number of arithmetic operations plays an important role in assessing the efficiency of the method. The calculation of the total number of arithmetic operations for both MsDTM and EMsDTM are divided into two parts. The first is to obtain the transformed functions by utilizing recurrence relation in each step and the second is to calculate the initial conditions at the end of each step in order to use them in the next step. These two stages only count the number of arithmetic operations. It is clear that the accuracy and computational effort of MsDTM highly rely on the capability of the approaches and the flexibility of the computer program.

Table 4 shows the values of $\propto_{jl}$, β_{jl}, δ_{jl} and ε_{jl} according to equations (18-21). Although the number of subintervals in MsDTM is set to 250, in EMsDTM it is decreased to 25. Furthermore, the number of series terms in EMsDTM for converging results is $m = 3$ while in MsDTM $N = 10$ has the same effect.

Table 4. Value of $\alpha_{ji}, \beta_{ji}, \delta_{ji}$ and ε_{ji} of EMsDTM for case study 1

$t\epsilon[0\ \ 50]$	$t\epsilon[50\ \ 100]$
$j=1$	$j=2$
$\alpha_{j1} = 6.541888e-7$	$\alpha_{j1} = 8.356483e-9$
$\alpha_{j2} = 0.0002902$	$\alpha_{j2} = -0.0000010$
$\alpha_{j3} = 0.0997090$	$\alpha_{j3} = -0.0001172$
$\beta_{j1} = -5.3697845$	$\beta_{j1} = -4.9009003$
$\beta_{j2} = -3.1149014$	$\beta_{j2} = -3.1246352$
$\beta_{j3} = -1.0367624$	$\beta_{j3} = -1.0366319$
$\delta_{j1} = 0$	$\delta_{j1} = 0.0000015$
$\delta_{j2} = 0$	$\delta_{j2} = -0.000287$
$\delta_{j3} = 0$	$\delta_{j3} = 0.0997307$
$\varepsilon_{j1} = -8.9110598$	$\varepsilon_{j1} = -4.900903$
$\varepsilon_{j2} = 2.8506968$	$\varepsilon_{j2} = -3.1246349$
$\varepsilon_{j3} = -2.2149804$	$\varepsilon_{j3} = -1.0366319$

Figure 3 shows the amplitude-time response of case study 1 calculated by EMsDTM, MsDTM and exact solution (Eq. (5)) over long periods of time. The solid blue line represents the EMsDTM solution with 2 subinterval computations and 650 arithmetic operations, the red dashed line denotes the MsDTM with 124 subinterval integration solution with 53,630 arithmetic operations. The number of arithmetic operations increases exponentially with an increasing the number of subintervals and terms. It is noted that the exact solution is derived for the system parameters $a = -0.446 + 0.397I$, $b = 1.446 - 0.397I$, $k = 0.792 - 1.468I$, $\omega = 0.050 - 0.370I$ and $\varphi = 0$ (see eq. (5)). Note that $I = \sqrt{-1}$.

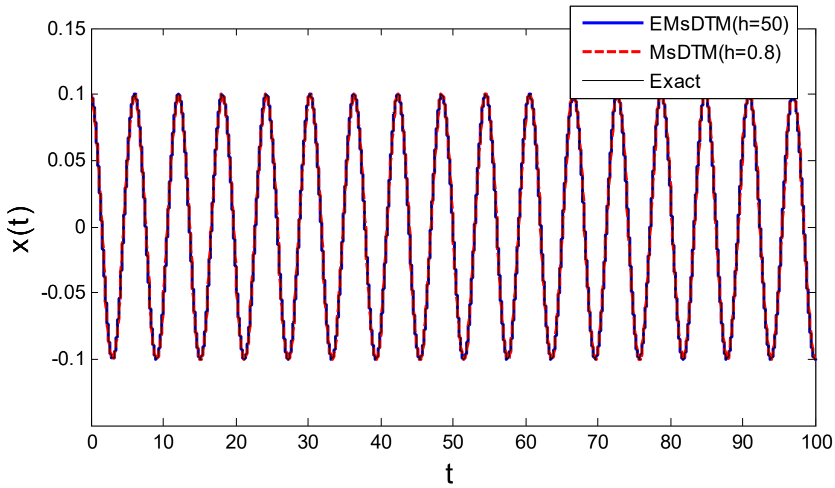

Fig. 3. Displacement solutions of for free undamped cubic-quintic Duffing equation for case study 1

The circular frequency value of 20.0000 obtained by EMsDTM exactly matches (0.1% tolerance) the closed-form solution. To compare the accuracy, Table 5 shows the absolute error values of EMsDTM for case study 1.

Table 5. The absolute EMsDTM error for free undamped cubic-quintic Duffing equation as a case study 1

t	$\lvert x(t)_{EMsDTM} - x(t)_{Exact}\rvert$	t	$\lvert x(t)_{EMsDTM} - x(t)_{Exact}\rvert$
0	0.0000	25	0.79428454 e-4
1	0.25108385 e-8	26	0.31121504 e-5
2	0.61604467 e-9	27	0.52853313 e-5
3	0.47328884 e-9	28	0.16564872 e-5
4	0.35165950 e-8	29	0.60198194 e-5
5	0.83082862 e-8	30	0.26297128 e-5
6	0.58526409 e-8	31	0.65407909 e-5
7	0.54972362 e-7	32	0.68921450 e-4
8	0.91719360 e-4	33	0.74815159 e-3
9	0.28583901 e-5	34	0.45054159 e-4
10	0.75720022 e-5	35	0.08382137 e-4
11	0.75372909 e-5	36	0.22897696 e-5
12	0.38044584 e-5	37	0.91333736 e-5
13	0.56782164 e-5	38	0.15237801 e-5
14	0.07585428 e-5	39	0.82581697 e-5
15	0.05395011 e-4	40	0.53834243 e-4
16	0.53079755 e-4	41	0.99613471 e-4
17	0.77916723 e-4	42	0.07817552 e-4
18	0.93401067 e-5	43	0.44267826 e-4
19	0.12990620 e-5	44	0.10665277 e-5
20	0.56882366 e-5	45	0.96189808 e-5
21	0.46939064 e-5	47	0.00463422 e-5
22	0.01190206 e-5	48	0.77491046 e-5
23	0.33712264 e-4	49	0.81730322 e-5
24	0.16218230 e-4	50	0.86869470 e-4

Figure 4 shows the velocity versus displacement for case study 1. In an undamped vibration system, no resistive force acts on the vibration object. Therefore, the energy of vibration does not change over time. This leads to an identical velocity-displacement diagram for all cycles. It can be seen that the results obtained by EMsDTM are in high harmony with the exact solution for case study 1.

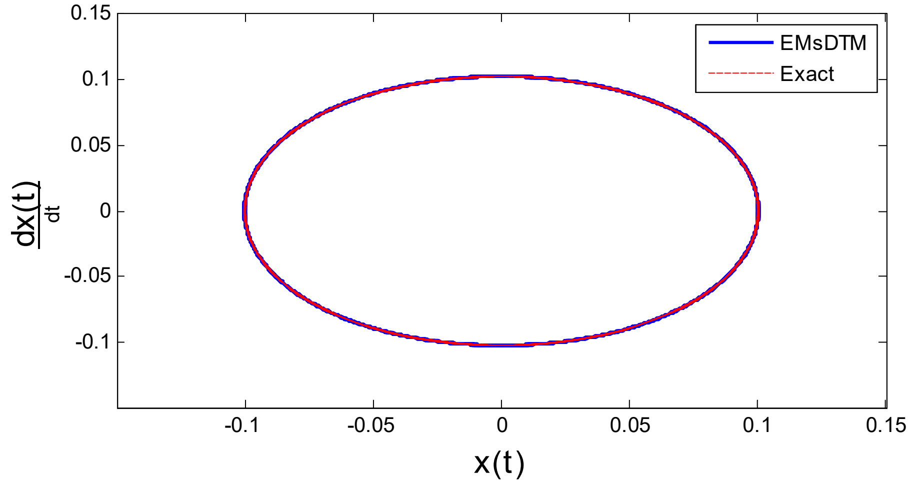

Fig. 4. Velocity-displacement diagram of free undamped vibration of cubic-quintic Duffing equation (case study 1)

4.1.2. Free undamped Duffing oscillator with seventh power and $A = 0.1$

In the case study 2 the Duffing oscillator has the following form:

$$\frac{d^2x(t)}{dt^2} + \rho_1 x(t) + \rho_3 x(t)^3 + \rho_5 x(t)^5 + \rho_7 x(t)^7 = 0, \tag{27}$$

where $\rho_1 = 1$, $\rho_3 = 10, \rho_5 = \rho_7 = 1$ and $A = 0.1$. In order to have accurate results, h must be selected 50. It means that the number of subintervals for $t \in [0 \ \ 100]$ is only 2 which is 55 times less than MsDTM with h=1.6. As illustrated in Fig. 5, the results of EMsDTM are compared to the numerical solution. It can be seen that the obtained results are quite matched to the numerical solution. Table 6 shows the values of $\propto_{jl}$, β_{jl}, δ_{jl} and ε_{jl}.

Table 6. Values of α_{ji}, β_{ji}, δ_{ji} and ε_{ji} for case study 2

$t\epsilon[0 \ \ 50]$	$t\epsilon[50 \ \ 100]$
$j = 1$	$j = 2$
$\alpha_{j1} = 7.2031e-8$	$\alpha_{j1} = 8.510939e-9$
$\alpha_{j2} = 0.0002902$	$\alpha_{j2} = 0.0000010$
$\alpha_{j3} = 0.0997091$	$\alpha_{j3} = -0.0001186$
$\beta_{j1} = -5.3722994$	$\beta_{j1} = -4.8978500$
$\beta_{j2} = -3.1149654$	$\beta_{j2} = -3.1248115$
$\beta_{j3} = -1.0367629$	$\beta_{j3} = -1.0366312$
$\delta_{j1} = 0$	$\delta_{j1} = 0.0000015$
$\delta_{j2} = 0$	$\delta_{j2} = -0.000287848$
$\delta_{j3} = 0$	$\delta_{j3} = 0.0997314$
$\varepsilon_{j1} = -8.911059$	$\varepsilon_{j1} = -4.8978534$
$\varepsilon_{j2} = 2.8506968$	$\varepsilon_{j2} = -3.1248112$
$\varepsilon_{j3} = -2.2149804$	$\varepsilon_{j3} = -1.0366312$

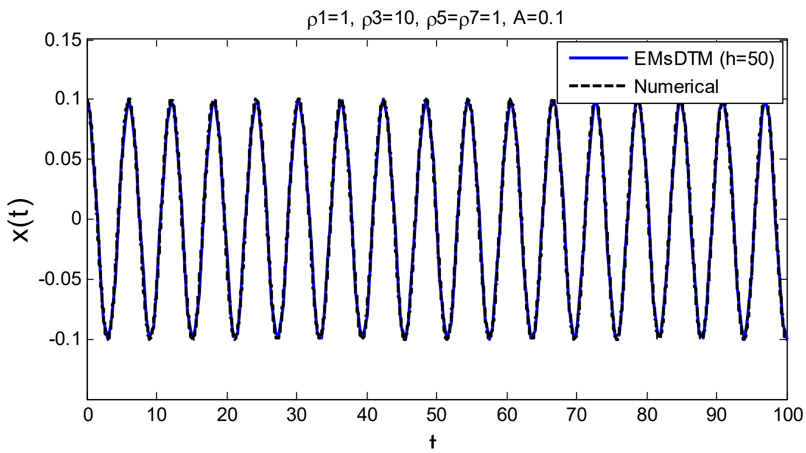

Fig. 5. Comparison of the EMsDTM (h=50) with Numerical solution for case study 2

4.1.3. Free undamped Duffing oscillator with seventh power and $A = 1$

For case study 3 n=7, $\rho_3 = 1, \rho_5 = 1, \rho_7 = 0.1$, and $A = 1$. Comparison of the solutions achieved by EMsDTM with numerical solutions is illustrated in Fig. 6. It can be seen that there is a great agreement between the analytical solutions as well as the numerical solutions. Table 7 shows the values of $\propto_{jl}$, β_{jl}, δ_{jl} and ε_{jl}. The number of subinterval for this example for $t \in [0\ \ 100]$, is 25 which is 50 times less than EMsDTM (h=0.2).

Table 7. Value of $\alpha_{ji}, \beta_{ji}, \delta_{ji}$ and ε_{ji} of EMsDTM for case study 3

$t\epsilon[0\ \ 4]$	$t\epsilon[4\ \ 8]$	$t\epsilon[8\ \ 12]$	...	$t\epsilon[96\ \ 100]$
$j = 1$	$j = 2$	$j = 3$	...	$j = 25$
$\alpha_{j1} = 0.000074$	$\alpha_{j1} = 0.000073$	$\alpha_{j1} = 0.000082$	...	$\alpha_{j1} = 0.000035 - 0.000010I$
$\alpha_{j2} = 0.017100$	$\alpha_{j2} = 0.016689$	$\alpha_{j2} = 0.0165261$	...	$\alpha_{j2} = 0.000035 + 0.000010I$
$\alpha_{j3} = 0.982825$	$\alpha_{j3} = 0.968516$	$\alpha_{j3} = 0.945529$	...	$\alpha_{j3} = 0.007686$
$\beta_{j1} = -13.116994$	$\beta_{j1} = -12.850207$	$\beta_{j1} = 12.064586$	...	$\beta_{j1} = 0.007686 - 4.709283I$
$\beta_{j2} = -5.962984$	$\beta_{j2} = -5.854240$	$\beta_{j2} = -5.604995$	...	$\beta_{j2} = -4.120832 - 4.709283I$
$\beta_{j3} = -1.588243$	$\beta_{j3} = -1.5664104$	$\beta_{j3} = -1.533125$	...	$\beta_{j3} = -1.077180$
$\delta_{j1} = 0$	$\delta_{j1} = -5.344645e - 7$	$\delta_{j1} = -0.0000062$	...	$\delta_{j1} = 0.000911 - 0.000589I$
$\delta_{j2} = 0$	$\delta_{j2} = 0.000135$	$\delta_{j2} = -0.001525$	...	$\delta_{j2} = -0.000911 + 0.0005\mathrm{I}$
$\delta_{j3} = 0$	$\delta_{j3} = 0.005103$	$\delta_{j3} = 0.057184$	...	$\delta_{j3} = -1.310203$
$\varepsilon_{j1} = -8.911059$	$\varepsilon_{j1} = -15.535257$	$\varepsilon_{j1} = -14.887018$	...	$\varepsilon_{j1} = 4.120800 - 4.709560\mathrm{I}$
$\varepsilon_{j2} = 2.850696$	$\varepsilon_{j2} = -7.572962$	$\varepsilon_{j2} = -7.293397$	...	$\varepsilon_{j2} = -4.120800 - 4.70956\mathrm{I}$
$\varepsilon_{j3} = -2.214980$	$\varepsilon_{j3} = -2.133214$	$\varepsilon_{j3} = -2.056662$	...	$\varepsilon_{j3} = -1.077150$

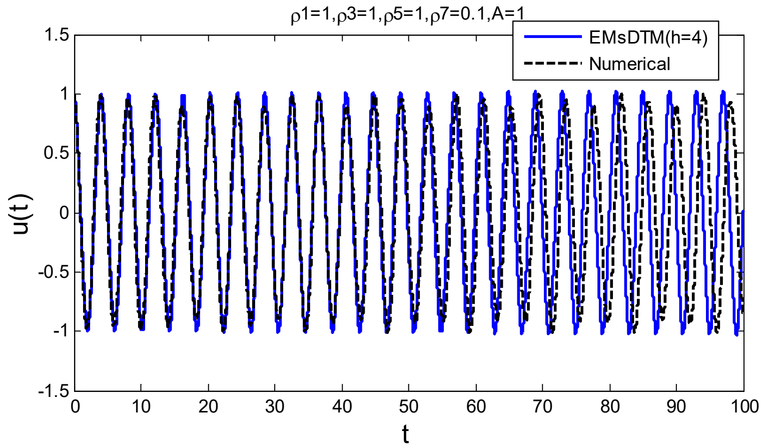

Fig. 6. Comparison of the EMsDTM (h=4) with numerical solution for case study 3

4.1.4. Free undamped Duffing oscillator with ninth power

The approximate solution for this case is illustrated in Fig. 7. To have accurate results, h needs to be set 50 which leads to have very fast and accurate solution compared to MsDTM. Table 8 shows the values of $\propto_{jl}$, β_{jl}, δ_{jl} and ε_{jl}.

Table 8. Value of $\alpha_{ji}, \beta_{ji}, \delta_{ji}$ and ε_{ji} of EMsDTM for case study 4

$t\epsilon[0\ \ 50]$	$t\epsilon[50\ \ 100]$
$j = 1$	$j = 2$
$\alpha_{j1} = 7.355483e - 7$	$\alpha_{j1} = 8.510939763e - 9$
$\alpha_{j2} = 0.000292$	$\alpha_{j2} = 0.000001032455547$
$\alpha_{j3} = 0.099706$	$\alpha_{j3} = -0.0001186693625$
$\beta_{j1} = -5.458258$	$\beta_{j1} = -4.897850045$
$\beta_{j2} = -3.119447$	$\beta_{j2} = -3.124811566$
$\beta_{j3} = -1.037047$	$\beta_{j3} = -1.036631293$
$\delta_{j1} = 0$	$\delta_{j1} = 0.000001513847481$
$\delta_{j2} = 0$	$\delta_{j2} = -0.0002878485321$
$\delta_{j3} = 0$	$\delta_{j3} = 0.09973149371$
$\varepsilon_{j1} = -8.911059862$	$\varepsilon_{j1} = -4.897853413$
$\varepsilon_{j2} = 2.850696882$	$\varepsilon_{j2} = -3.124811260$
$\varepsilon_{j3} = -2.214980447$	$\varepsilon_{j3} = -1.036631297$

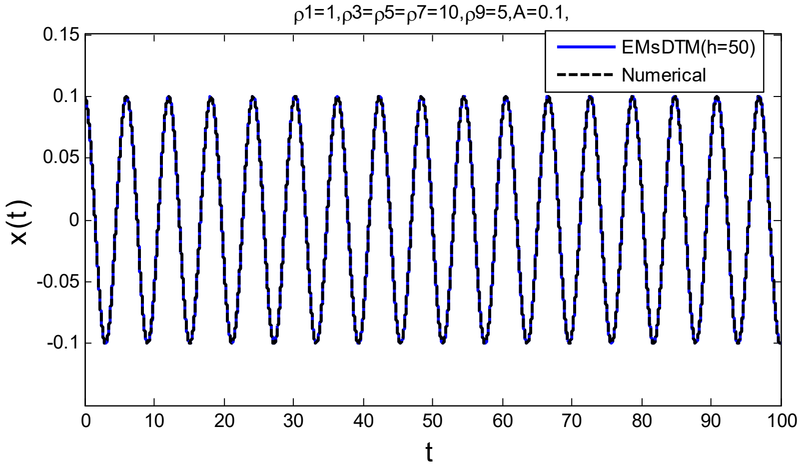

Fig. 7. Comparison of the EMsDTM (h=50) with numerical solution for case study 4

4.2. Damped cubic-quintic Duffing oscillator

In this section the free damped and force damped cubic-quintic Duffing oscillator are through investigated.

4.2.1. Free damped cubic-quintic Duffing oscillator

The free damped cubic–quintic Duffing oscillator equation is given by:

$$\frac{d^2x(t)}{dt^2} + \rho_1 x(t) + \mu\frac{dx(t)}{dt} + \rho_3 x(t)^3 = 0, \qquad with\ x(0) = A, x'(0) = 0. \tag{28}$$

As mentioned previously, μ represents the damping parameter. According to Table 1 and Eq. (16), the differential transformation of Eq. (27) for each subinterval is:

$$\begin{aligned} X_j[i+2] = -\frac{1}{(i+2)(i+1)}\Bigg(& X_j[i] + \mu(i+1)X_j[i+2] + \rho_3 \sum_{k_2=0}^{i}\sum_{k_1=0}^{k_2} X_j[k_1]X_j[k_2-k_1]X_j[i-k_2] \\ & + \rho_5 \sum_{k_4=0}^{i}\sum_{k_3=0}^{k_4}\sum_{k_2=0}^{k_3}\sum_{k_1=0}^{k_2} X_j[k_1]X_j[k_2-k_1]X_j[(k_3-k_2)]X_j[(k_4-k_3)]X_j[(i-k_4)]\Bigg) \end{aligned} \tag{29}$$

To further assess the accuracy of EMsDTM, the damped cubic-quintic Duffing oscillator (Eq. (28)) is considered with parameters $\rho_1 = 1, \rho_3 = 10, \rho_5 = 1, \mu = 0.01$, with the initial conditions of $x(0) = 0.1$ and $x'(0) = 0$. In order to get accurate results for MsDTM, h needs to be set equal to 0.2 while for EMsDTM h=5 gives reasonable results .Table 8 shows the values of $\propto_{jl}, \beta_{jl}, \delta_{jl}$ and ε_{jl} according to equations (18-21).

Table 9. Value of $\alpha_{ji}, \beta_{ji}, \delta_{ji}$ and ε_{ji} of EMsDTM for free damped cubic-quintic Duffing oscillator as case study 5

$t\epsilon[0\ \ 5]$	$t\epsilon[5\ \ 10]$	$t\epsilon[10\ \ 15]$	...	$t\epsilon[95\ \ 100]$
$j = 1$	$j = 2$	$j = 3$	...	$j = 25$
$\alpha_{j1} = 6.359782e-7$	$\alpha_{j1} = 8.3455e-7$	$\alpha_{j1} = -1.299707e-12$	...	$\alpha_{j1} = -6.604186e-8$
$\alpha_{j2} = 0.0002895$	$\alpha_{j2} = -0.0002691$	$\alpha_{j2} = 0.0002515$	...	$\alpha_{j2} = -0.0000713$
$\alpha_{j3} = 0.0997097$	$\alpha_{j3} = 0.0448037$	$\alpha_{j3} = -0.0566332$	...	$\alpha_{j3} = -0.0624205$
$\beta_{j1} = -5.381907006$	$\beta_{j1} = -5.0174829$	$\beta_{j1} = -14.7520569$	...	$\beta_{j1} = -5.1884367$
$\beta_{j2} = -3.1164110$	$\beta_{j2} = -3.1253755$	$\beta_{j2} = -3.0954996$	...	$\beta_{j2} = -3.0510451$
$\beta_{j3} = -1.0367786$	$\beta_{j3} = -1.0450245$	$\beta_{j3} = -1.0274052$	...	$\beta_{j3} = -1.0151838$
$\delta_{j1} = 4.3653551e-7$	$\delta_{j1} = 0.0000011$	$\delta_{j1} = 8.5878762e-7$	...	$\delta_{j1} = 9.5491656e-9$
$\delta_{j2} = 0.0007187$	$\delta_{j2} = 0.0000527$	$\delta_{j2} = -0.0000856$	...	$\delta_{j2} = 0.0000208$
$\delta_{j3} = -0.0013392$	$\delta_{j3} = -0.0874349$	$\delta_{j3} = -0.0773344$	...	$\delta_{j3} = 0.00648859$
$\varepsilon_{j1} = -4.2614288$	$\varepsilon_{j1} = -4.8418610$	$\varepsilon_{j1} = -5.0769648$	...	$\varepsilon_{j1} = -5.7271760$
$\varepsilon_{j2} = -1.278319299$	$\varepsilon_{j2} = -2.862050192$	$\varepsilon_{j2} = -3.059987566$	...	$\varepsilon_{j2} = -3.059902872$
$\varepsilon_{j3} = -0.6874097864$	$\varepsilon_{j3} = -1.033272973$	$\varepsilon_{j3} = -1.037742976$	...	$\varepsilon_{j3} = -0.9638366727$

Figure 8 plots the solutions obtained for the free damped cubic-quintic Duffing oscillator with EMsDTM and numerical. It can clearly be seen from Fig. 8 that all solutions are nearly the same for most of the interval shown. It should be noted that h is chosen to be 0.2 for MsDTM, while $h = 1$ for EMsDTM to give the same results.

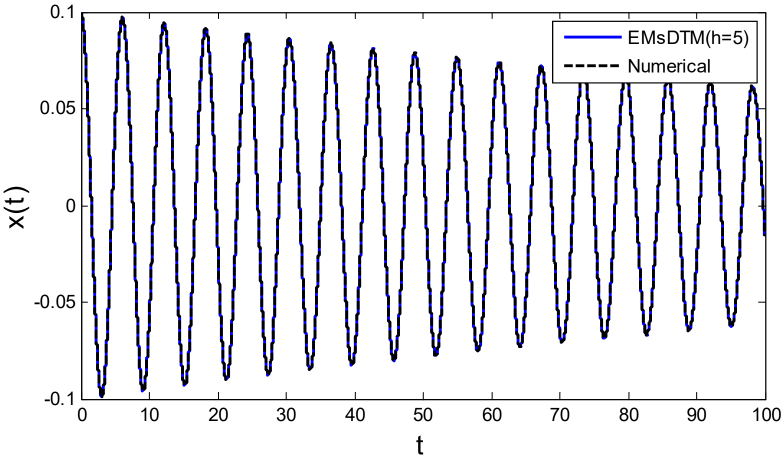

Fig. 8. Displacement solution of case free damped cubic-quintic Duffing equation as case study 5

4.2.2. Forced damped cubic-quintic Duffing oscillator

In this section, the solutions of forced cubic-quintic Duffing oscillators by EMsDTM and MsDTM are compared with the numerical result. The driven, damped cubic-quintic Duffing oscillator with a single sinusoidal forcing is given by:

$$\frac{d^2x(t)}{dt^2}+\rho_1 x(t)+\mu\frac{dx(t)}{dt}+\rho_3 x(t)^3+\rho_5 x(t)^5=f cos\Omega t \tag{30}$$

The differential transformation of equation (30) for each subinterval is:

$$\begin{aligned}X_j[i+2]=-\frac{1}{(i+2)(i+1)}\Bigg(&\rho_1 X_j[i]+\mu(i+1)X_j[i+1]+\rho_3\sum_{k_2=0}^{i}\sum_{k_1=0}^{k_2}X_j[k_1]X_j[k_2-k_1]X_j[i-k_2]\\&+\rho_5\sum_{k_4=0}^{i}\sum_{k_3=0}^{k_4}\sum_{k_2=0}^{k_3}\sum_{k_1=0}^{k_2}X_j[k_1]X_j[(k_2-k_1)]X_j[(k_3-k_2)]X_j[(k_4-k_3)]X_j[(i-k_4)]\\&-\frac{f}{i!}cos\left(\frac{\pi i}{2}\right)\Bigg).\end{aligned} \tag{31}$$

In case study 6, $\rho_1=1,\ \mu=0.01,\ \rho_3=\rho_5=0.1,\ f=0.01$ and $\Omega=1$ are considered. Figure 9 illustrates the effect of subinterval h on convergence. The obtained results are compared with the numerical method. Based on Fig. 9, h should be secure to 0.05 for MsDTM which gives the number of subintervals $j=2000$. By choosing $h=1$ and using EMsDTM the number of subintervals and series terms are considerably decreased.

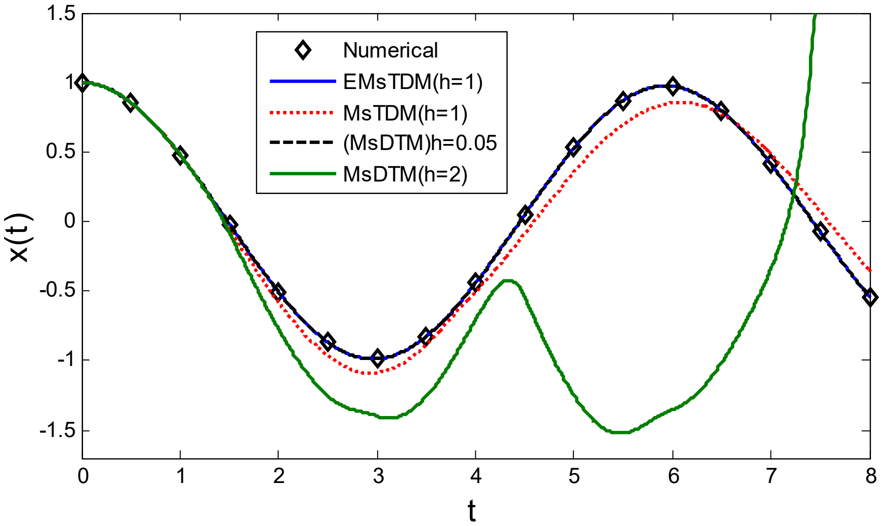

Fig. 9. Effect of subinterval h on result accuracy of MsDTM and EMsDTM for case study 6

Figure 10 presents the displacement solutions with MsDTM, EMsDTM and numerical. The response of the physical system is extremely well-behaved and repeatable. Although the results obtained with MsDTM and EMsDTM have good agreement with the numerical method, the number of arithmetic operations for MsDTM and EMsDTM for the damped

Duffing equation are around 365,000 and 9,250, respectively. Furthermore, the number of subintervals for MsDTM is 100 times higher than for EMsDTM. Due to the high number of MsDTM subintervals, the computation of the solution takes considerable time.

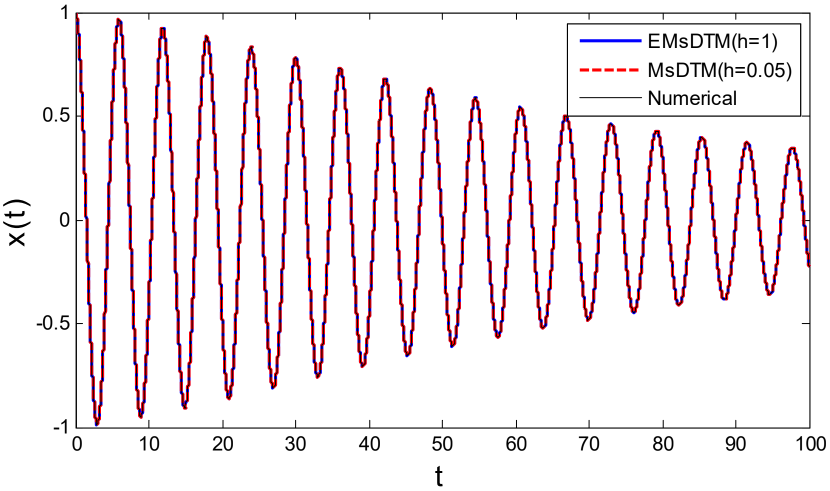

Fig. 10. Displacement solution of case study 6

Table 10. Value of $\alpha_{ji}, \beta_{ji}, \delta_{ji}$ and ε_{ji} of EMsDTM for forced vibration (case study 6)

$t\epsilon[0\ \ 1]$	$t\epsilon[1\ \ 2]$	$t\epsilon[2\ \ 3]$		$t\epsilon[49\ \ 50]$
$j=1$	$j=2$	$j=3$	...	$j=50$
$\alpha_{j1}=0.000057$	$\alpha_{j1}=0.000240$	$\alpha_{j1}=-0.000082$	...	$\alpha_{j1}=-0.0000323$
$\alpha_{j2}=0.005212$	$\alpha_{j2}=0.005816$	$\alpha_{j2}=0.005422$	...	$\alpha_{j2}=-0.000428$
$\alpha_{j3}=0.994730$	$\alpha_{j3}=0.485814$	$\alpha_{j3}=-0.507219$	...	$\alpha_{j3}=0.503799$
$\beta_{j1}=-6.490978$	$\beta_{j1}=-5.146781$	$\beta_{j1}=-5.533677$	...	$\beta_{j1}=-4.986169$
$\beta_{j2}=-3.473227$	$\beta_{j2}=-3.282148$	$\beta_{j2}=-3.216616$	...	$\beta_{j2}=-2.997133$
$\beta_{j3}=-1.063327$	$\beta_{j3}=-1.045477$	$\beta_{j3}=-1.078615$	...	$\beta_{j3}=-1.006230$
$\delta_{j1}=0.001600$	$\delta_{j1}=0.0000037$	$\delta_{j1}=0.000039+0.000035I$	...	$\delta_{j1}=-6.439010e-7$
$\delta_{j2}=5.36917e-7$	$\delta_{j2}=0.000296$	$\delta_{j2}=-0.000039+0.00003I$	...	$\delta_{j2}=0.001127$
$\delta_{j3}=0.000935$	$\delta_{j3}=0.857239$	$\delta_{j3}=0.832152$	...	$\delta_{j3}=0.374872$
$\varepsilon_{j1}=-1.232490I$	$\varepsilon_{j1}=-7.265116$	$\varepsilon_{j1}=5.719696-1.009840I$	...	$\varepsilon_{j1}=-6.496077$
$\varepsilon_{j2}==-6.938384$	$\varepsilon_{j2}=-5.09327-$	$\varepsilon_{j2}=-5.719696-1.00984I$	...	$\varepsilon_{j2}=-2.995178$
$\varepsilon_{j3}=-2.104993$	$\varepsilon_{j3}=-1.067869$	$\varepsilon_{j3}=-6.774907$	...	$\varepsilon_{j3}=-1.025985$

Figure 11 shows velocity versus displacement for damped vibration of the cubic-quintic Duffing equation (see eq. (28)). Damped vibration refers to vibration where the vibrating object loses its energy to the surroundings over time. Therefore, contrary to undamped vibration, the velocity-displacement diagram for each cycle varies. In other words, with increasing time, the velocity and displacement are decreased. As can be seen, the results obtained with EMsDTM match the numerical results of numerical.

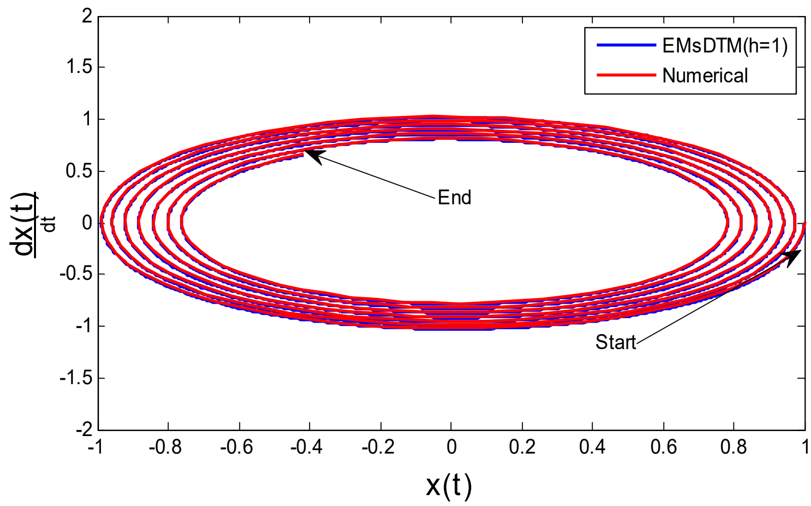

Fig. 11. Velocity-displacement diagram of case study 6

Table 11 shows the absolute error of EMsDTM with the numerical solution for this example. The maximum error is less than 0.22% in the time 33. Hence, the proposed method is suitable for solving damped vibration of the cubic-quintic Duffing equation.

Table 11. The absolute of EMsDTM for case study 6

t	$\lvert x(t)_{EMsDTM} - x(t)_{RK4}\rvert$	t	$\lvert x(t)_{EMsDTM} - x(t)_{RK4}\rvert$
0	0.0000	25	0.43886997 e-4
1	0.37860938 e-8	26	0.11111922 e-4
2	0.81158045 e-8	27	0.25806469 e-3
3	0.53282558 e-7	28	0.40871984 e-5
4	0.35072710 e-8	29	0.59489607 e-3
5	0.93900156 e-8	30	0.26221174 e-3
6	0.87594281 e-8	31	0.60284308 e-5
7	0.55015634 e-8	32	0.71121578 e-4
8	0.62247508 e-7	33	0.22174673 e-3
9	0.58704470 e-7	34	0.11741765 e-5
10	0.20774229 e-7	35	0.29667587 e-5
11	0.30124633 e-7	36	0.31877830 e-5
12	0.47092334 e-7	37	0.42416675 e-4
13	0.23048816 e-3	38	0.50785828 e-3
14	0.84430879 e-4	39	0.08551579 e-4
15	0.19476428 e-4	40	0.26248223 e-5
16	0.22592178 e-4	41	0.80101462 e-5
17	0.17070804 e-4	42	0.02922027 e-5
18	0.22766429 e-5	43	0.92885413 e-5
19	0.43569868 e-5	44	0.73033086 e-5
20	0.31110228 e-5	45	0.48860897 e-4
21	0.92337964 e-3	47	0.57852506 e-4
22	0.43020739 e-4	48	0.23728357 e-3
23	0.18481632 e-5	49	0.45884882 e-5
24	0.90488096 e-5	50	0.96308853 e-4

5. Conclusion

Duffing oscillation is one of the paradigms of nonlinear dynamics. In this research, a very efficient method called EMsDTM based on the well-known MsDTM method is thoroughly investigated for solving an unforced, undamped cubic-quintic Duffing oscillator and forced cubic-quintic Duffing oscillator with a single sinusoidal forcing term. By employing EMsDTM, a simple and accurate technique with less subintervals and arithmetic operations than MsDTM, the frequency and solutions are obtained for both small and large amplitudes of oscillation. The certain value conditions of the system parameters in the three case studies presented in this paper yield fairly good agreement with the exact solutions for free vibration and the RK4 numerical approach for forced vibration. It is shown that the present method is very effective, convenient and more accurate in solving a strongly cubic–quintic Duffing oscillator.

Conflict of Interest

The authors declared no potential conflicts of interest with respect to the research, authorship and publication of this article.

Funding

The authors received no financial support for the research, authorship and publication of this article.

References

[1] U. Starossek, Exact analytical solutions for forced undamped Duffing oscillator, *International Journal of Non-linear Mechanics*, 85 (2016) 197-1206.

[2] S. Yong-Jun, W. Shao-Fang, Y. Shao-Pu, G. Shu-Qi, L. Lin-Ru, Analytical threshold for chaos in a Duffing oscillator with delayed feedbacks, *International Journal of Non-linear Mechanics*, 98 (2018) 173-179.

[3] Ludeke C. A., Wagner W. S., The generalized Duffing equation with large damping, *International Journal of Non-linear Mechanics*, 3 (1968) 383-395.

[4] M. RafikovI, J. M. BalthazarII, Â. M. Tusset, An optimal linear control design for nonlinear systems, *Journal of the Brazilian Society of Mechanical Sciences and Engineering*, 30 (4) 2008 1806-3691.

[5] A. Elias-Zuniga, O. Martinez-Romero, R.K. Cordoba-Diaz, Approximate solution for the Duffing-harmonic oscillator by the enhanced cubication method, *Mathematical Problems in Engineering*, 2012 (2012) Article ID 618750.

[6] M. Abdur Razzak, An analytical approximate technique for solving cubic–quintic Duffing oscillator, *Alexandria Engineering Journal*, 55 (2016) 2959–2965.
[7] S.K. Lai, C.W. Lim, B.S. Wu, C. Wang, Q.C. Zeng, X.F. He, Newton-harmonic balancing approach for accurate solutions to nonlinear cubic–quintic Duffing oscillators, *Applied Mathematical Mo*delling, 33 (2) (2009) 852–866.
[8] F. Saadi, M.J. Azizpour, S.A. Zahedi, Analytical solutions of Kortweg-de Vries (KdV) equation, *World Academy of Science, Engineering and Technology,* 69 (2010) 171-175.
[9] Z. Yan, A new sine–Gordon equation expansion algorithm to investigate some special nonlinear differential equations, *Chaos, Solitons and Fractals*, 23 (3) (2005) 767–775.
[10] S. Lenci, G. Menditto, A.M. Tarantino, Homoclinic and heteroclinic bifurcations in the non-linear dynamics of a beam resting on an elastic substrate, *International Journal of Non-linear Mech*anics, 34 (4) (1999) 615–632.
[11] A.I. Maimistov, Propagation of an ultimately short electromagnetic pulse in a nonlinear medium described by the fifth-order Duffing model, *Physical and Quantum Optics*, 94 (2) (2003) 251–257.
[12] I. Kovacic, M.J. Brennan, *The Duffing equation: nonlinear oscillators and their be*havior, Wiley, Chichester, West Sussex, UK; Hoboken, 2011.
[13] H. Hu, E.H. Dowell, L.N. Virgin, Resonances of a harmonically forced Duffing oscillator with time delay state feedback, *Nonlinear Dynamic*, 15 (1998) 311-327.
[14] K.S. Mendelson, Perturbation theory for damped nonlinear oscillators, *Journal of Mathematical Physics*, 2 (1970) 3413-3415.
[15] A. Fereidoon, S.A. Zahedi, D.D. Ganji, Y. Rostamiyan, Homotopy Perturbation method to solving nonlinear WBK equations, *Far East Journal of Dynamical Systems*, 10 (2) (2008), 239-254.
[16] M. Alinia, G. Domairry, M. Gorji, A. Zahedi, S. Soleimani, Analysis on viscoelastic fluid flow and heat transfer over a stretching sheet, *International Journal for Computational Methods in Engineering Science and Mechanics*, 12(6) (2011) 278-289.
[17] K. Parand, M. Delkhosh, An efficient numerical solution of nonlinear Hunter–Saxton equation, *Communications in Theoretical Physics*, 67 (2017) 483–492.
[18] M. Kazemnia, S.A. Zahedi, M. Vaezi, N. Tolou, Assessment of modified variational iteration method in BVPs high-order differential equations, *Journal of Applied Sciences*, 8(22) (2008) 4192-4197.
[19] S.A. Zahedi, M. Fazeli, N. Tolou, Analytical solution of time-dependent non-linear partial differential equations using HAM, HPM and VIM, *Journal of Applied Sciences*, 8(16) (2008) 2888-2894.
[20] D.D. Ganji, A. Sadighi, I. Khatami, Assessment of two analytical approaches in some nonlinear problems arising in engineering sciences, *Physics Letters A*, 372(24) (2008) 4399-4406.
[21] M. Fazeli, S.A. Zahedi, N. Tolou, Explicit solution of nonlinear fourth-order parabolic equations via homotopy perturbation method, *Journal of Applied Sciences*, 8(14) (2008) 2619-2624.
[22] T. Pirbodaghi, S.H. Hoseini, M.T. Ahmadiana, G.H. Farrahi, Duffing equations with cubic and quintic nonlinearities, *Computers and Mathematics with Applications*, 57 (2009) 500–506.
[23] I. Hashim, Adomian decomposition method for solving BVPs for fourth-order integro-differential equations, *Journal of Computational and Applied Mathematics*, 193 (2006) 658–664.
[24] S.K. Lai, C.W. Lim, B.S. Wu, C. Wang, Q.C. Zeng, X.F. He, Newton-harmonic balancing approach for accurate solutions to nonlinear cubic-quintic Duffing oscillators, *Applied Mathematical M*odelling, 33 (2) (2008) 852-866.
[25] Z. Guo, A.Y.T. Leung, H.X. Yang, Iterative homotopy harmonic balancing approach for conservative oscillator with strong odd-nonlinearity, *Applied Mathematical Mo*delling, 35 (4) (2011) 1717-1728.
[26] Panayotounakos, D.E., Theotokoglou, E.E. and Markakis M.P., Exact analysis solutions for the unforced damped duffing nonlinear oscillator, *Comptes Rendus – Mechanics*, 334 (2006) 311-316.
[27] Y. Farzaneh, A.A. Tootoonchi, Global error minimization method for solving strongly nonlinear oscillator differential equations, *Journal of Computers and Mathematics with Applications*, 59 (8) (2010) 2887-2895.
[28] A. Elias-Zuniga, Exact solution of the cubic-quintic Duffing oscillator, *Applied Mathematical Modelling*, 37 (2013) 2574–2579.
[29] M. Malik, H.H. Dang, Vibration analysis of continuous system by differential transformation, *Applied Mathematics and Computation*, 96(1) (1998) 17–26.
[30] M. Keimanesh, M.M. Rashidi, A.J. Chamkha, R. Jafari, Study of a third grade non-Newtonian fluid flow between two parallel plates using the multi-step differential transform method, *Computers and Mathematics with Applications*, 62(8) (2011) 2871-2891.
[31] A. Gökdoğan, M. Merdan, A. Yildirim, Adaptive multi-step differential transformation method to solving nonlinear differential equations, *Mathematical and Computer Modelling*, 55(3-4) (2012) 761-769.

[32] M. Hatami, M. Sheikholeslami, G. Domairry, High accuracy analysis for motion of a spherical particle in plane Couette fluid flow by multi-step differential transformation method, *Powder Technology*, 260 (2014) 59-67.
[33] Z. M. Odibat, C. Bertelle, M.A. Aziz-Alaoui, G. H.E. Duchamp, A multi-step differential transform method and application to non-chaotic or chaotic systems, *Computers and Mathematics with Applications*, 59 (2010) 1462-1472.
[34] M. Nourifar, A. A. Sani, A. Keyhani, Efficient multi-step differential transform method: theory and its application to nonlinear oscillators, *Communications in Nonlinear Science and Numerical Simulation*, 53 (2017) 154-183.